

# Effect of Horizontal Nonuniformity of Diabatic Heating on Tropical Cyclone Intensity and Structure\*

YU Hui<sup>1,2</sup> (余 晖), DUAN Yihong<sup>2</sup> (端义宏), and LIANG Xudong<sup>2</sup> (梁旭东)

<sup>1</sup>*Nanjing University of Information Science and Technology, Nanjing 210044*

<sup>2</sup>*Shanghai Typhoon Institute, Shanghai 200030*

(Received February 14, 2004; revised December 14, 2004)

## ABSTRACT

The effect of the horizontal variation of diabatic heating on the tropical cyclone intensity and structure is studied in this paper. According to the potential vorticity (PV) equation in axis-symmetric cylindrical coordinates, PV disturbance caused by the radial difference of diabatic heating is positive (negative) inside (outside) the maximum heating radius, implying that the radial nonuniformity of diabatic heating should contribute positively to the intensity of a tropical cyclone while negatively to its size.

A primitive equation model is then used to get some quantitative ideas on the problem. Results show that the modeled tropical cyclone weakens by about 20% but is larger in size if the effect of horizontal variety of convective heating is excluded in thermodynamic and dynamic equations. The PV disturbance originated from the horizontal nonuniformity of diabatic heating is positive inside the maximum heating radius and negative outside, in consistent with the PV equation analyses. The maximum disturbance (both negative and positive) appears around the maximum heating level and their magnitude is comparable to that generated by vertical variance of heating. It is concluded that the effect of the horizontal heat nonuniformity on the intensity and structure of TC cannot be neglected.

**Key words:** tropical cyclone, intensity, structure, diabatic heating

---

## 1. Introduction

Much attention has been paid to the role played by diabatic heating in the genesis and intensification of tropical cyclone (TC). Based on a two-dimensional primitive equation model, Li (1984) proposed that the evolution of TC should be different if the maximum heating appears at different height. Yang et al. (1995) found that abrupt intensification of TC at the mid-latitudes is closely related to the vertical structure of convective heating. May and Holland (1998) suggested that the potential vorticity produced by the vertical gradient of heating from the stratified precipitation around a TC plays a very important role in the intensity change of the TC. Murara and Jenu (2000) further addressed the problem using a high resolution spectrum model. Most of these studies focus on the vertical variance of diabatic heating due to the fact that vertical gradient of diabatic heating generally contributes much more than its horizontal gradient to the

generation of potential vorticity.

However, while studying the effect of the spacial inhomogeneity of deep convective heating on the dynamic features of subtropical atmosphere, Liu et al. (2001) found that there is a deep negative vorticity forcing to the north of a heating region even though no diabatic heating exists there, because the horizontal gradient of convective heating is not equal to zero. Such a result shows that effects of the horizontal variance of diabatic heating on the atmospheric circulation are not neglectable. For TC, the most intense convection happens in its eyewall region and there are ascending and descending flows alternatively in the spiral cloud region. Therefore, the horizontal scale of convective heating is usually small, which implies that the horizontal gradient of diabatic heating can be very large and may have notable effects on TC intensity and structure. This paper is a preliminary study on this problem.

---

\*Sponsored by the National Natural Science Foundation of China under Grant Nos. 49975014, 40275018 and 40333025.

## 2. Qualitative analysis

The PV equation can be written as

$$\frac{dP}{dt} = \alpha \zeta_a \cdot \nabla Q, \quad (1)$$

where  $P = \alpha \zeta_a \cdot \nabla \theta$  is potential vorticity (PV),  $\alpha$  is specific volume,  $\theta$  is potential temperature,  $Q$  is diabatic heating and  $\zeta_a$  is absolute vorticity. The frictional term has been omitted in Eq.(1).

In the cylindrical coordinate  $(r, \varphi, z)$  with origin at TC center, Eq.(1) could be written as

$$\frac{dP}{dt} = \alpha \zeta_r \frac{\partial Q}{\partial r} + \alpha \frac{\zeta_\varphi}{r} \frac{\partial Q}{\partial \varphi} + \alpha \zeta_z \frac{\partial Q}{\partial z}. \quad (2)$$

Here,  $\zeta_r, \zeta_\varphi$  and  $\zeta_z$  are three components of absolute vorticity in  $r, \varphi$  and  $z$  directions, respectively. We have

$$\begin{aligned} \zeta_r &= \frac{1}{r} \left( \frac{\partial w}{\partial \varphi} - \frac{\partial r v_\varphi}{\partial z} \right) + f_1 \sin \varphi, \\ \zeta_\varphi &= \frac{\partial v_r}{\partial z} - \frac{\partial w}{\partial r} + f_1 \cos \varphi, \\ \zeta_z &= f + \frac{\partial v_\varphi}{\partial r} - \frac{1}{r} \frac{\partial v_r}{\partial \varphi} + \frac{v_\varphi}{r}, \end{aligned}$$

where  $v_r, v_\varphi$ , and  $w$  are three components of wind velocity. The parameters  $f_1$  and  $f$  are Coriolis parameters.

For simplicity, only axis-symmetric TC is considered here. In an axis-symmetric coordinate, Eq.(2) can be simplified as

$$\frac{dP}{dt} = \alpha \zeta_z \frac{\partial Q}{\partial z} + \alpha \zeta_r \frac{\partial Q}{\partial r}. \quad (3)$$

Here,

$$\zeta_r = -\frac{\partial v_\varphi}{\partial z} + f_1 \sin \varphi, \quad \zeta_z = f + \frac{\partial v_\varphi}{\partial r} + \frac{v_\varphi}{r}.$$

The two terms on the right side of Eq.(3) are PV disturbance generated by vertical and radial gradients of  $Q$  respectively.

### 2.1 Contribution of radial variance of $Q$

The second term on the right side of Eq.(3) represents the contribution of radial non-uniformity of  $Q$  to PV disturbance, which is determined by both  $\zeta_r$  and radial gradient of  $Q$ .

Generally speaking, TC's tangential velocity ( $v_\varphi$ ) decreases with height in the free atmosphere and  $\zeta_r$

is positive. Thus PV disturbance generated by radial gradient of  $Q$  should be zero at maximum heating radius  $R_{\max}^{\text{heat}}$  (which usually exists in eyewall or spiral bands), negative outside and positive inside. While in the lower part of boundary layer, tangential velocity ( $v_\varphi$ ) increases with height sharply and  $\zeta_r$  should be negative, hence PV disturbance should be negative inside  $R_{\max}^{\text{heat}}$  and positive outside.

The distribution of PV disturbance generated by radial gradient of  $Q$  is shown schematically in Fig.1.

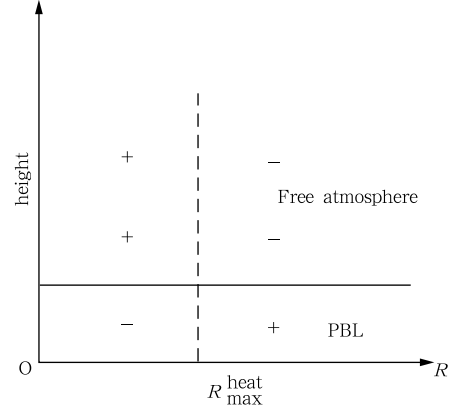


**Fig.1.** Schematic chart for PV disturbance generated by radial gradient of  $Q$ . Abscissa: radius, ordinate: height, o: TC center,  $R_{\max}^{\text{heat}}$ : maximum heating radius.

### 2.2 Contribution of vertical variance of $Q$

The first term on the right side of Eq.(3) represents the contribution of vertical nonuniformity of  $Q$  to PV disturbance, which is determined by both  $\zeta_z$  and vertical gradient of  $Q$ .

Inside a TC,  $\zeta_z$  is generally positive, thus PV disturbance generated by the vertical gradient of  $Q$  should be zero at the maximum heating height  $H_{\max}^{\text{heat}}$ , negative upward and positive downward. This is shown schematically in Fig.2.

According to the above analyses, diabatic heating can generate PV disturbance because it is not homogeneous spatially, including both the vertical non-uniformity, which has long been paid great attention, and the horizontal variety. In the free atmosphere, the radial variance of  $Q$  can generate positive PV disturbance inside the maximum heating radius, which

contributes positively to TC's intensity, and negative outside, which may cause TC to contract. Nevertheless, it remains unknown whether these PV disturbances can compare with that generated by  $Q$ 's vertical variance. Therefore, a primitive equation model is employed to get some quantitative ideas.

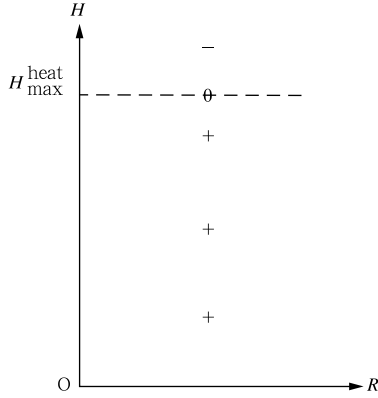


**Fig.2.** Schematic chart for PV disturbance generated by vertical gradient of  $Q$ . Abscissa: radius, ordinate: height, o: TC center,  $H_{\max}^{\text{heat}}$ : maximum heating radius.

### 3. Model description and experiment design

The model is based on primitive equations in  $\sigma$  coordinates (Anthes et al., 1987).

$$\begin{aligned} \frac{\partial P^* u}{\partial t} = & -m^2 \left( \frac{\partial P^* u u / m}{\partial x} + \frac{\partial P^* v u / m}{\partial y} \right) \\ & - \frac{\partial P^* u \dot{\sigma}}{\partial \sigma} - m P^* \left[ \frac{R T_v}{(P^* + P_t / \sigma)} \frac{\partial P^*}{\partial x} \right. \\ & \left. + \frac{\partial \phi}{\partial x} \right] + f P^* v + F_H u + F_V u, \end{aligned} \quad (4)$$

$$\begin{aligned} \frac{\partial P^* v}{\partial t} = & -m^2 \left( \frac{\partial P^* u v / m}{\partial x} + \frac{\partial P^* v v / m}{\partial y} \right) \\ & - \frac{\partial P^* v \dot{\sigma}}{\partial \sigma} - m P^* \left[ \frac{R T_v}{(P^* + P_t / \sigma)} \frac{\partial P^*}{\partial y} \right. \\ & \left. + \frac{\partial \phi}{\partial y} \right] - f P^* u + F_H v + F_V v, \end{aligned} \quad (5)$$

$$\begin{aligned} \frac{\partial P^*}{\partial t} = & -m^2 \left( \frac{\partial P^* u / m}{\partial x} + \frac{\partial P^* v / m}{\partial y} \right) \\ & - \frac{\partial P^* \dot{\sigma}}{\partial \sigma}, \end{aligned} \quad (6)$$

$$\frac{\partial \phi}{\partial \ln(\sigma + P_t / P^*)} = -R T_v, \quad (7)$$

$$\begin{aligned} \frac{\partial P^* T}{\partial t} = & -m^2 \left( \frac{\partial P^* u T / m}{\partial x} + \frac{\partial P^* v T / m}{\partial y} \right) \\ & - \frac{\partial P^* T \dot{\sigma}}{\partial \sigma} + \frac{R T_v \omega}{C_{pm}(\sigma + P_t / P^*)} + \frac{L_V}{C_{pm}} \\ & \cdot N_h(\sigma)(1-b)gM_t + F_H T + F_V T, \end{aligned} \quad (8)$$

$$\begin{aligned} \frac{\partial P^* q_v}{\partial t} = & b g M_t N_m(\sigma) + V_{gf}(\sigma) \\ & + F_H q_v + F_V q_v, \end{aligned} \quad (9)$$

where  $u$  and  $v$  are horizontal wind components,  $\phi$  the geopotential height,  $T$  temperature,  $q_v$  specific humidity, and  $T_v$  virtual temperature.  $P^* = P_s - P_t$  with  $P_s$  surface pressure and  $P_t$  model top pressure.  $\dot{\sigma} = d\sigma/dt$ .  $F_H$  and  $F_V$  are horizontal and vertical diffusion terms respectively.  $\omega = dP/dt$ .  $M_t$  is the total moisture ratio, with  $b$  the percentage in  $M_t$  for moistening the air to be cloudy.  $N_h(\sigma)$  and  $N_m(\sigma)$  are vertical distribution functions for convective heating and water.  $V_{gf}(\sigma)$  is the vertical eddy flux convergence of water vapor in cumulus convection. Others are all commonly-used symbols.

There are 15 levels vertically and the  $\sigma$  levels are placed at values of 1.0, 0.98, 0.95, 0.90, 0.8, 0.65, 0.5, 0.4, 0.32, 0.26, 0.20, 0.15, 0.10, 0.06, 0.03, and 0.0. The Kuo cumulus parameterization (Kuo, 1974) scheme and the bulk aerodynamic model of the planetary boundary layer following Deardorff (1972) are employed.

The model domain is 5000 km  $\times$  5000 km with a horizontal grid size of 50 km. The "Arakawa B" horizontal grid structure is used with the inflow/outflow lateral boundary conditions.  $\dot{\sigma}$  is set to zero at  $\sigma = 0$  and 1. All the variables are defined at the half- $\sigma$  levels except  $\dot{\sigma}$ .

A bogus TC is specified by the radius of 15 m s<sup>-1</sup> winds ( $R_{15}$ ), the boundary radius of the TC ( $R_E$ ) and the central pressure ( $P_C$ ). The sea-level pressure at a distance  $r$  from the TC center,  $P_{SE}(r)$ , is given by Fujita's (1952) formula

$$P_{SE}(r) = P_E - \Delta P \left[ 1 + \left( \frac{r}{R_0} \right)^2 \right]^{-0.5},$$

where  $P_E$  is the environmental pressure,  $R_0$  the radius of maximum wind, and  $\Delta P = P_E - P_C$ .

Two experiments (Exp.A and Exp.B) are carried out on  $f$ -plane in a quiescent environment.

At the initial time in Exp.A, the atmosphere is homogeneous at the standard pressure levels (1000, 850, 700, 500, 300, 200, and 100 hPa). Vertical temperature structure is obtained from the ECMWF re-analysis data (00UTC 21 September 1990) averaged within  $10^\circ$ - $20^\circ$ N and  $135^\circ$ - $155^\circ$ E. Humidity values are set to 90%, 85%, 80%, 50%, 20%, 20%, and 10% at the 7 standard pressure levels from 1000 to 100 hPa, respectively. The geopotential heights at various pressure levels are calculated using the hydrostatic relationship. The model SST (lower boundary condition) is assumed to be homogeneous at  $28^\circ$ C. Coriolis parameter is set as constant with a value equal to that at  $20^\circ$ N. Initial parameters of TC,  $R_{15}$  and  $P_C$ , are set to 450 km and 990 hPa respectively.

Exp.B is mostly the same as Exp.A, except that the effects of horizontal inhomogeneity of convective heating are neglected. This is done as follows. At time level  $t$ , two temperature tendency terms are calculated according to thermodynamic Eq.(8). One is the real tendency, while the other is obtained by ignoring convective heating (see Eq.(10)). Thus, we have two temperature fields for time level  $t + 1$ . One is the real temperature  $T$ . The other is exclusive of convective heating, which is defined as  $T'$ . As computing elements at time level  $t + 2$ ,  $T'$  is used in the advection term of thermodynamic equation to remove the effect of horizontal nonuniformity of convective heating on temperature tendency. Besides, geopotential height  $\phi'$  is calculated using  $T'$  and then substituted into dynamic equations to compute the terms related to the horizontal gradient of geopotential height. Thus, the effect of horizontal variance of convective heating on wind field can be neglected approximately.

$$\begin{aligned} \frac{\partial P^*T}{\partial t} = & -m^2 \left( \frac{\partial P^*uT/m}{\partial x} + \frac{\partial P^*vT/m}{\partial y} \right) \\ & - \frac{\partial P^*T\dot{\sigma}}{\partial \sigma} + \frac{RT_v\omega}{C_{pm}(\sigma + P_t/P^*)} \\ & + F_H T + F_V T. \end{aligned} \quad (10)$$

#### 4. Diagnosis of model results

With pressure being the vertical coordinate, the

PV equation can be written as

$$\frac{dP}{dt} = -g(\zeta_p + f)Q_p - g\mathbf{k} \times \frac{\partial \mathbf{v}}{\partial p} \cdot \nabla_p Q, \quad (11)$$

where

$$\zeta_p = \left( \frac{\partial v}{\partial x} - \frac{\partial u}{\partial y} \right)_p, \quad Q_p = \frac{\partial Q}{\partial p}.$$

The first (second) term on the right side of Eq. (11) represents PV disturbance due to the vertical (horizontal) gradient of diabatic heating. Figures 3a and 3b depict  $x - z$  cross-sections of these two terms through TC center for Exp.A at 48h, and Fig.3c depicts the sum of the two terms.

Figure 3a shows that PV disturbance generated by vertical inequality of convective heating is positive below the maximum heating height (about 200-300 hPa), but negative above it, which is a well-known fact.

In Fig.3b, on two sides of the TC center, PV disturbance aroused by the horizontal variance of convective heating is positive inside the maximum heating radius and negative outside, consistent with the qualitative analyses in Section 2. The disturbance extrema appear around maximum heating height with values comparable to those in Fig.3a. Thus, PV disturbances generated by horizontal heating inequality are not negligible. Another notable thing in Fig.3b is that there are alternating regions of negative and positive disturbance horizontally, because there are several heating extrema that might be related to spiral rain bands in the TC.

According to Fig.3c, the horizontal heating variance not only contributes positively to the total PV generation near the center, but also causes positive regions to extend upward above the maximum heating height. Besides, negative PV areas aloft expand notably compared with that in Fig.3a. These are all favorable conditions for the intensification of TC. Because of the contribution from horizontal heating variety, the PV disturbance is not uniquely positive below the maximum heating height as in Fig.3a, while it is alternately positive and negative horizontally as in

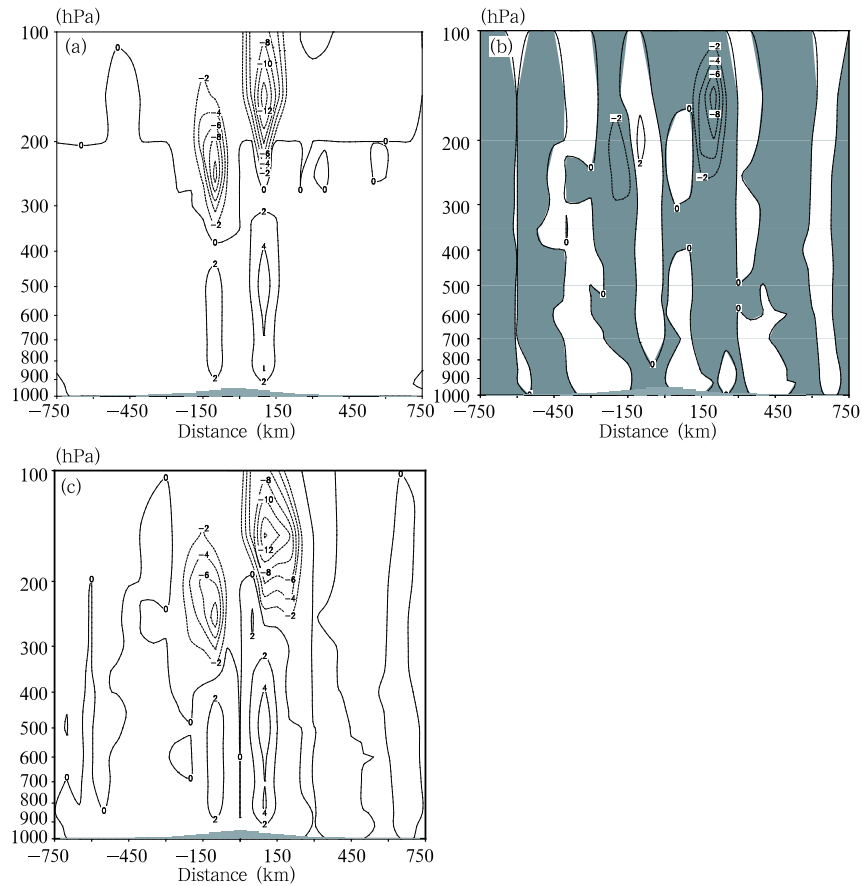


**Fig.3.**  $x - z$  cross-sections of PV disturbances generated by vertical (a) and horizontal (b) gradients of convective heating through TC center, and the sum (c) of them. Here the abscissa represents the distance to TC center (km), the unit of PV disturbance is in  $10^{-10} \text{ m}^{-2} \text{ s}^{-2} \text{ K kg}^{-1}$ .

Fig.3c.

Now, let us see the effects of horizontal inhomogeneity of convective heating on TC intensity and structure separately.

#### 4.1 Intensity

In both Exp.A and Exp.B, TC strengthens continuously (Fig.4). To hour 48, the minimum central pressure falls by 40 hPa in Exp.A. Exp.B gets a much weaker TC with central pressure falling only by 32 hPa in 48 hours, about 80% of Exp.A. It is obvious that the positive contribution of horizontal heating nonuniformity to TC's intensity can not be ignored.

#### 4.2 Structure

According to the PV difference between hours 36 and 48 of Exp.A (Fig.5), positive PV increases around the center and negative PV aloft develops, which are

both consistent with the fact that TC deepens.

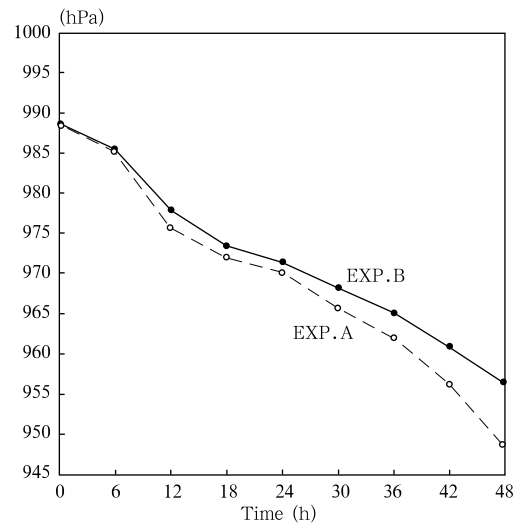


**Fig.4.** Intensity changes of TC in Exp.A (dashed line) and Exp.B (dotted line).

Another notable thing is that the positive disturbance is concentrated within the area of about 150 km radius and there is negative disturbance outside that radius, implying that the modeled TC does contract as it intensifies.

PV difference between Exp.A and Exp.B at 48h (Exp.B minus Exp.A, Fig.6) shows that the positive PV of Exp.B around the center is less than that of Exp.A, which is consistent with TC intensity's decrease. Horizontally, these differences are negative and positive alternately. The positive difference outside

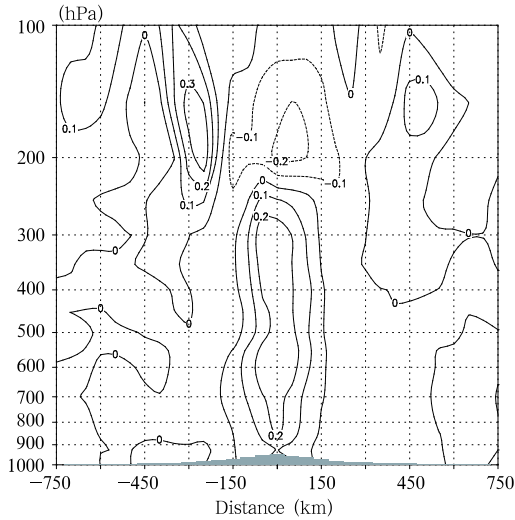


**Fig.5.** As in Fig.3, but for PV difference between hours 36 and 48 in Exp.A.

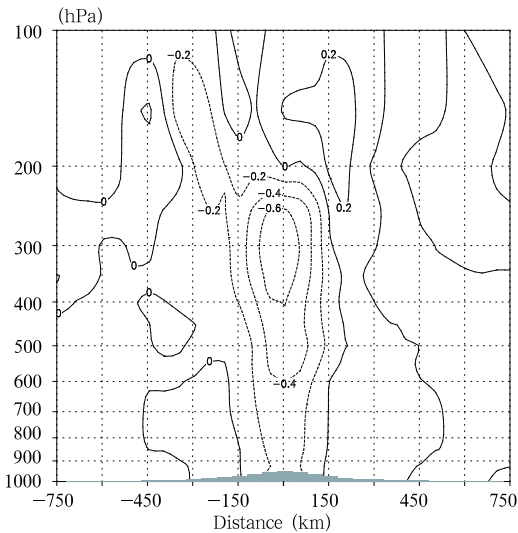


**Fig.6.** As in Fig.3, but for PV difference between Exp.A and Exp.B at 48h.

the negative area over TC center suggests that TC in Exp.B has a larger area of positive PV around the center than that in Exp.A.

Willoughby et al. (1982) have studied the contraction phenomenon of TC. As they pointed out, the observed inward motion of convective rings stems from the asymmetry between thermally direct and indirect gyres. A condensational heat source near the tangential wind maximum induces both large total subsidence outward from the wind maximum and smaller total subsidence inward from the maximum. On the outside, the subsidence is distributed over a wide area; on the inside, it is concentrated near the heat source. The subsidence-induced adiabatic warming is stronger radially inward from the ring, so that a sharp contrast of hydrostatic isobaric height falls forms across the wind maximum. Through the gradient wind relation, the tangential wind increases most rapidly at and just inward from the maximum. This explanation only takes the effect of secondary circulation into account, but neglects the role of heat source itself. The horizontal nonuniformity of diabatic heating may be another factor responsible for TC contracting.

## 5. Conclusion and discussion

The effect of the horizontal variation of diabatic heating on the tropical cyclone intensity and structure is studied in this paper. According to the potential vorticity (PV) equation in axis-symmetric cylindrical coordinates, PV disturbance caused by radial difference of diabatic heating is positive (negative) inside (outside) the maximum heating radius, implying that the radial nonuniformity of diabatic heating should contribute positively to the intensity of a tropical cyclone while negatively to its size.

To get some quantitative ideas, a primitive equation model is then used to address the problem for idealized tropical cyclones on  $f$ -plane. Results show that the modeled tropical cyclone weakens by about 20% but is larger in size if the effect of horizontal variety of convective heating is excluded in thermodynamic and dynamic equations. The PV disturbances due to the horizontal difference of heating are positive

inside the maximum heating radius and negative outside, which is consistent with the PV equation analyses. The maximum PV disturbances (both negative and positive) appear around the maximum heating level and their magnitude is comparable to that generated by the vertical variance of heating. Horizontal difference of heating not only intensifies positive PV disturbances around tropical cyclone center, but also makes it extending upward above the maximum heating level, and meanwhile, the negative disturbance area aloft enlarges. Below the level of maximum heating, the total PV disturbance caused by spacial variance of heating is not evenly positive, but in alternately positive and negative distribution horizontally due to horizontal difference of heating.

All the facts mentioned above suggest that the effect of horizontal heat nonuniformity on the intensity and structure of TC cannot be neglected. However, this is just a preliminary study with only an idealized TC considered in a low resolution model. The strong heating near TC center has a horizontal scale of about 150 km in this study, which should be much smaller in reality, implying a much larger horizontal heating gradient. The existence of spiral rain band should be the reason for several heating maxima away from the TC center, while the relationship between them is not clear yet. In addition, the effects of environmental flow,  $\beta$ -effect, asymmetric structure, and so on, are left out here. These all need further studies.

## REFERENCES

Anthes, R. A., E. -Y. Hise, and Y. -H. Kuo, 1987: Description of the Penn State/NCAR mesoscale model

version 4 (MM4). NCAR Tech. Note NCAR/TN-282, National Center for Atmospheric Research, Boulder, Colorado, 66 pp.

Deardorff, J. W., 1972: Parameterization of the planetary boundary layer for use in general circulation model. *Mon. Wea. Rev.*, **100**, 93-106.

Fujita, T., 1952: Pressure distribution in typhoon. *Geophys. Mag.*, **23**, 437-452.

Kuo, H. -L., 1974: Further studies of the parameterization of the influence of cumulus convection on large-scale flow. *J. Atmos. Sci.*, **31**, 1232-1240.

Li Congyin, 1984: A numerical study on tropical depression development—the effect of condensation heat profile. *Tropical Meteorology*, **1**, 24-31. (in Chinese)

Liu Yimin, Wu Guoxiong, et al., 2001: Thermal adaptation, overshooting, dispersion, and subtropical anticyclone II: Horizontal inhomogeneous heating and energy dispersion. *Chinese Journal of Atmospheric Sciences*, **25**(3), 317-328. (in Chinese)

May, Peter T., and Holland Greg J., 1998: The role of potential vorticity generation in tropical cyclone rainbands. Symp. On Tropical Cyclone. 95-97.

Murata Akihiko, and Ueno Mitsuru, 2000: A case study of tropical cyclone intensity forecast depending on cumulus parameterization. The 24th Conference on Hurricanes and Tropical Meteorology. 234-235.

Willoughby, H. E., J. A. Clos, and M. G. Shoreibah, 1982: Concentric Eye walls, secondary wind maxima, and the evolution of the hurricane vortex. *J. Atmos. Sci.*, **39**, 395-411.

Yang Yuanqin, et al., 1995: Numerical study on the sensitivity of factors affecting erratic motion and abrupt intensity change of typhoon. In: Studies on Scientific, Operational Experiment and Synoptic Dynamics Theory of Typhoon, 104-111. (in Chinese)